Electronic intraband scattering in a transition-metal dichalcogenide observed by double-excitation ultrafast electron diffraction

Yui Iwasaki,[1,a)] Takumi Fukuda,[2,a)] Godai Noyama,[1] Mizuki Akei,[1] Hidemi Shigekawa,[3] Paul J. Fons,[4] Muneaki Hase,[3] Yusuke Arashida,[3,b)] and Masaki Hada,[3,5,c)]

[1]*College of Engineering Sciences, University of Tsukuba, Tsukuba 305-8573, Japan*

[2]*Graduate School of Pure and Applied Sciences, University of Tsukuba, Tsukuba 305-8573, Japan*

[3]*Institute of Pure and Applied Sciences, University of Tsukuba, Tsukuba 305-8573, Japan*

[4]*Faculty of Science and Technology, Keio University, Yokohama 223-8522, Japan*

[5]*Tsukuba Research Center for Energy Materials Science (TREMS), University of Tsukuba, Tsukuba 305-8573, Japan*

The electronic dynamics in the excited state of transition-metal dichalcogenides (TMDs) has attracted great interest. To understand the ultrafast intraband scattering process of excited electrons in the conduction band, we demonstrated ultrafast time-resolved electron diffraction measurements with double-optical-pulse excitation and ultrafast transient reflectivity measurements of a TMD material, 2H-$MoTe_2$. Due to the saturable absorption (or Pauli blocking) effect present in 2H-$MoTe_2$, the system does not absorb the second excitation pulse until the excited electrons generated by the first excitation pulse with a specific fluence are scattered in the conduction band. By exploiting the Pauli blocking effect in ultrafast time-resolved electron diffraction measurements with double-optical-pulse excitation, we found that the excited electrons were scattered within 100 fs comparable to the excitation optical pulse duration. Furthermore, the excited electrons relaxed to the lowest energy level of the conduction band (K- or Σ-valley) within 1–2 ps.

Transition-metal dichalcogenides (TMDs) are two-dimensional layered materials of transition-metal and chalcogen atoms.[1–5] The dynamics of the excited electrons in the conduction band of TMDs have particularly attracted attention in optoelectronics and quantum information since valley-selective electronic excitation can be realized in this class of materials.[6–11] The excited electrons relax in terms of both momentum and energy to lower energy valleys in the conduction band[12,13] under the restriction of the lattice (phonon), charge, and spin degrees of freedom. The scattering process regarding momentum relaxation occurs mainly through fast elastic electron–electron interactions. The scattering process in energy relaxation occurs mainly through inelastic electron–electron and electron–lattice interactions. Time-resolved angle-resolved photoemission spectroscopy (Tr-ARPES) and two-photon photoemission (2PPE) spectroscopy have been used to directly observe the electronic scattering of

a) Y. Iwasaki and T. Fukuda contributed equally to this work.

b) Author to whom correspondence should be addressed. Electronic mail: arashida.yusuke.kb@u.tsukuba.ac.jp

c) Author to whom correspondence should be addressed. Electronic mail: hada.masaki.fm@u.tsukuba.ac.jp

excited electrons in the conduction band.[14,15] However, observing the electronic scattering of excited electrons in the conduction band with the other pump-probe methodologies has been quite challenging because, for example, optical pump-optical probe methods are more sensitive to interband transition between the valence and conduction bands, and these interband phenomena interfere with the electronic scattering signal within the band.[16–18] A complementary method to observe the electronic scattering of excited electrons is important for further understanding and exploring the excited state dynamics of TMDs.

Here, we propose to observe the ultrafast electronic scattering of excited electrons in the conduction band of a TMD material, 2H-$MoTe_2$, by using ultrafast time-resolved electron diffraction measurements[19,20] with double-optical-pulse excitation in the Pauli blocking regime. Saturable absorption is a representative third-order nonlinear optical effect in which light transmission linearly increases above a certain light intensity via the Pauli blocking effect.[21] A nonlinear optical response is useful not only in the photonics field but also in the material science field. Photoinduced phase transition,[22,23] homogeneous melting,[24–26] and laser ablation,[27,28] represent nonlinear optical effects used in materials science. Saturable absorption is directly applied for mode-locked lasers.[29–31] In a previous study, we observed saturable absorption effect for a 2H-$MoTe_2$ thin film at an incident fluence of 4–12 mJ/cm^2.[32] The critical carrier density for Pauli blocking corresponds to approximately 0.4% of valence electrons. This fluence range for saturable absorption is suitable for our ultrafast time-resolved electron diffraction measurements with double-optical-pulse excitation; therefore, we chose a 2H-$MoTe_2$ thin film for the target material. In the present study, we found that the excited electrons were scattered in 2H-$MoTe_2$ within 100 fs and relaxed to the lowest energy level of the conduction band (K- or Σ-valley) within 1–2 ps by combining ultrafast time-resolved electron diffraction measurements with double-optical-pulse excitation and ultrafast transient reflectivity measurements.

The experimental setup for ultrafast time-resolved electron diffraction is shown in **Fig. 1**. Ultrafast time-resolved electron diffraction measurements were performed on an ultrathin 2H-$MoTe_2$ film with a pump wavelength of 400 nm under vacuum conditions. A femtosecond laser with a central wavelength of 800 nm, a repetition rate of 1 kHz, and a pulse duration of ~100 fs was used for ultrafast time-resolved electron diffraction.[33,34] An optical pump pulse with a wavelength of 400 nm was generated by second harmonic generation (SHG) from a beta barium borate (BBO) crystal. The optical pump pulse was doubled by a Mach–Zehnder interferometer (indicated by a dotted red square in **Fig. 1**). The pulse interval between the optical pump pulses was adjusted by the optical stage. The optical pump pulses were focused onto the sample with a diameter of 360 μm. The pulse duration of an optical pump pulses was approximately 100 fs and the incident fluence was 5 mJ/cm^2. The acceleration voltage of the electron probe pulse (~1 ps) was 75 kV and the diameter of the electron beam was 100 μm. The sample preparation method is shown in supplementary material (Fig. S1).

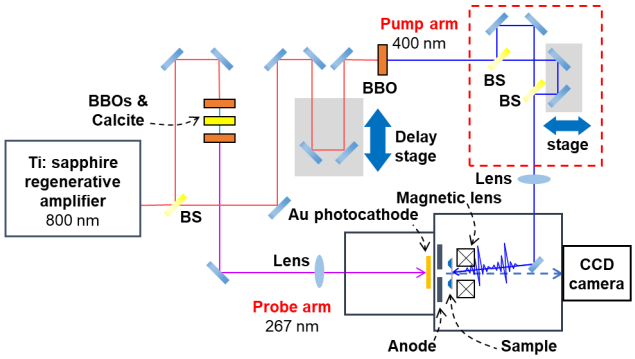

FIG. 1. Experimental setup for double pulse excitation ultrafast time-resolved electron diffraction. BS and CCD are beam splitter and charge coupled device, respectively. A dashed red box represents a Mach–Zehnder interferometer to generate double-excitation pulse.

Ultrafast transient reflectivity measurements were performed on bulk 2H-$MoTe_2$ with a pump wavelength of 400 nm and a probe wavelength of 400 nm under ambient conditions. The ultrafast transient reflectivity measurement was conducted using a femtosecond-pulsed laser source with a central wavelength of 800 nm, a repetition rate of 100 kHz, and a pulse duration of ~45 fs. A 400-nm pump pulse was generated by SHG from a β-BBO crystal. The spot diameter of the pump and probe light were approximately 20 μm. The sample used in the reflectivity measurement was a bulk 2H-$MoTe_2$ sample with a thickness of approximately 100 μm.

Figure 2(a) shows the calculated band structure of bulk 2H-$MoTe_2$. The electronic structure of bulk 2H-MoTe2 was generated using the plane-wave density-functional theory program VASP 6.42.[35] Projector augmented waves were used as the basis.[36] The generalized gradient approximation (GGA) in the form of PBESol (PBE) was used.[37] A value of 520 eV was used for the energy cutoff based on a convergence study that yielded a tolerance of 1 meV in total energy. An 8×8×2 Monkhorst-Pack grid was used for Brillouin zone integration. Spin-orbit coupling was enabled. According to the band structure, the 400 nm (3.1 eV) excitation photons can excite electrons at almost all momenta in the band structure. Schematic illustrations of ultrafast time-resolved electron diffraction measurements with double-optical-pulse excitation in the Pauli blocking regime are shown in **Figs. 2(b)** and **2(c)**. **Figure 2(b)** shows the case in which the pulse interval of the two optical pulses (t_{pi}) is longer than the time constant of the electronic scattering of excited electrons in the conduction band (τ). In this condition, the first optical pulse excites an electron from the valence band to the conduction band, and the photoexcitation level is sufficient to induce the saturable absorption effect. Electronic scattering occurs in the conduction band on the timescale of τ. Subsequently, the second optical pulse again excites an electron from the valence band to the conduction band, where the Pauli blocking effect

does not occur since the previously excited electron is no longer in the same state. The electron probe pulse observes the thermal effects induced by the absorbed light through the Debye–Waller factor. Ultrafast time-resolved electron diffraction measurements have been widely used for this class of materials.[38–42] In contrast, when t_{pi} is shorter than τ, as shown in **Fig. 2(c)**, the system does not absorb the second pulse due to the Pauli blocking effect. For this experiment, the time resolution of the system is not determined by the duration of the electron probe pulse but by the duration of the two excitation optical pulses. Note that the incident fluence used for this study is below the damage threshold, and we find no structural phase transition or damage signature in this study, such as that for ablation and tellurium segregation.[43]

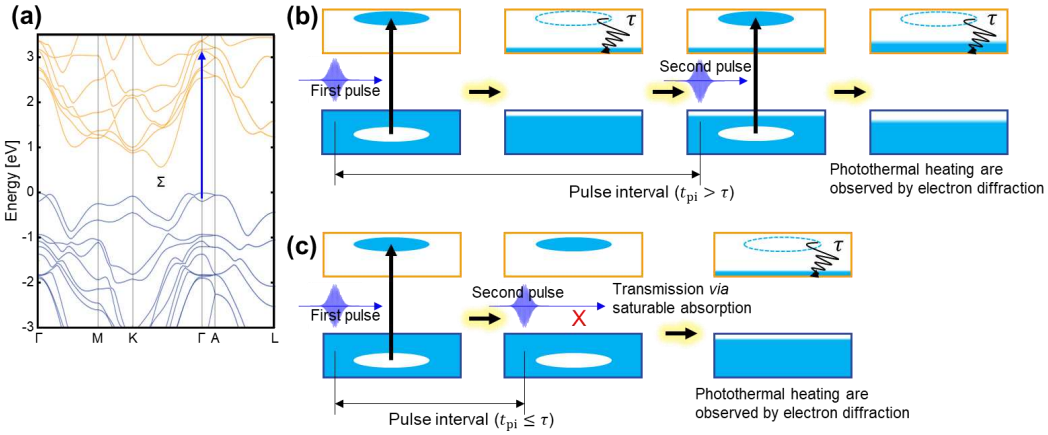

FIG. 2. (a) Calculated band structure of 2H-$MoTe_2$. The blue arrow shows a representative electron transition of 400-nm (3.1 eV) excitation. Schematic illustrations of ultrafast time-resolved electron diffraction measurements with double-optical-pulse excitation in the Pauli block regime. The cases of $t_{pi} > \tau$ (b) and $t_{pi} < \tau$ (c).

Figure 3(a) shows the electron diffraction pattern from a 40-nm-thick 2H-$MoTe_2$ single crystal. The electron diffraction shows a sixfold symmetric pattern with diffraction spots from the {100}, {110}, and {200} planes. **Figure 3(b)** shows the intensity changes of the 110 diffraction spots under single-pulse and double-pulse (t_{pi} = 20 ps) photoexcitation. The intensity changes of the other diffraction spots are provided in Fig. S2. The intensity changes of the diffraction spots under single-pulse photoexcitation show the same behavior as in a previous report.[32] The intensity decreases after photoexcitation at approximately 10 ps due to the thermal (Debye–Waller) effect. As shown in the figure, the intensity under double-pulse photoexcitation decreases by twofold compared to that under single-pulse photoexcitation, which suggests that the second pulse was absorbed in the sample without the Pauli blocking effect at a t_{pi} of 20 ps, as shown in **Fig. 2(a)**. To estimate the time constant of the electronic scattering of excited electrons in the conduction band (τ), we measured the diffraction intensity changes for different

pulse intervals of the two optical pulses, as shown in **Fig. 3(c)**. Because the interference pattern of two pulses induces strong instability at t_{pi} = 0 ps, we used single-pulse excitation of 10 mJ/cm^2 instead of double-pulse excitation of 5 mJ/cm^2 at t_{pi} = 0 ps. As shown in the figure, the intensity decreases for t_{pi} = 0 and 0.1 ps are relatively low compared to those for t_{pi} > 0.2 ps. For t_{pi} > 0.2 ps, the intensity decreases show a similar tendency to that for t_{pi} = 20 ps. This suggests that the second pulses with t_{pi} = 0 and 0.1 ps are in the Pauli blocking regime, as shown in **Fig. 2(b)**, and that the electronic scattering of excited electrons in the conduction band has already occurred for t_{pi} > 0.2 ps. The intensity changes of other diffraction spots for t_{pi} values of 0–20 ps are provided in Fig. S3. We can estimate τ using the intensity change as a function of t_{pi}, as shown in **Fig. 3(d)**. An exponential fit to the data in **Fig. 3(d)** yield a value of τ ≈ 100 fs. Since the pulse duration of the excitation pulse was approximately 100 fs, we can conclude that the time constant of the electronic scattering of excited electrons in the conduction band should be less than 100 fs. This result corresponds well to the previously reported time constants obtained by Tr-ARPES and 2PPE spectroscopy.[44–46]

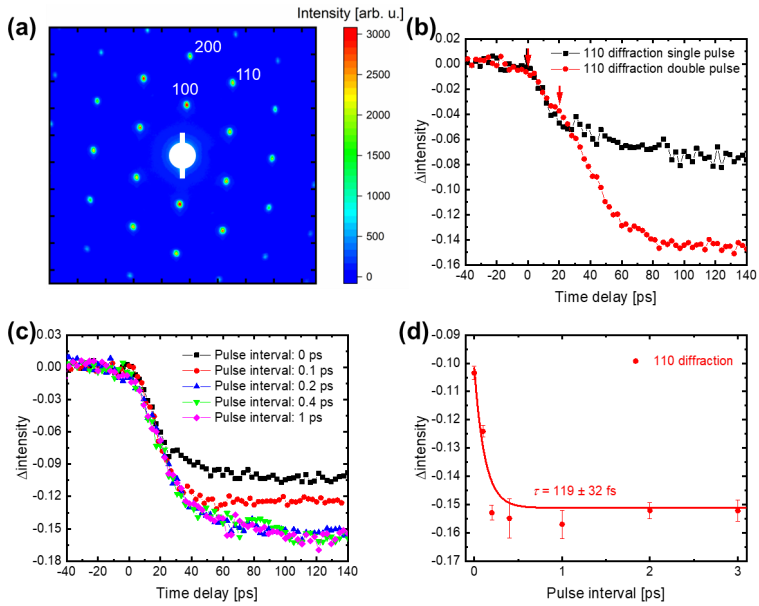

FIG. 3. Ultrafast time-resolved electron diffraction measurements of 2H-$MoTe_2$ with two-pulse excitation. (a) Electron diffraction pattern from a single-crystalline 2H-$MoTe_2$ thin film. (b) Intensity changes of the 110 diffraction spots under single-pulse and double-pulse (t_{pi} = 20 ps) photoexcitation. The black and red arrows show the excitation time points. (c) Intensity changes of the 110 diffraction spots for various pulse intervals of the two optical pulses. (d) Intensity change of the 110 diffraction spot as a function of t_{pi}.

Comparing the results of the ultrafast time-resolved electron diffraction measurements with those of ultrafast transient reflectivity measurements is worthwhile. We discuss the 400-nm optical pump and single 400-nm optical probe measurements at an incident fluence of 5 mJ/cm^2, as shown in **Fig. 4**. In the 400-nm-pump and 400-nm-probe measurements, the transient reflectivity can trace the electronic dynamics accompanying the interband transition, scattering, and relaxation at all momenta in the band structure of 2H-$MoTe_2$. As shown in the figure, a sharp decrease, relaxation, and a long-lived component are observed. We performed time-domain fit using a decreasing function (step-like error function: $\theta(t;\tau_{s1}) = [\mathrm{erf}(t/\tau_{s1}) + 1]/2$), a damping (exponential decay) function, and a rising long-lived component with a step-like error function [$\theta(t;\tau_{s2})$]:

$$y(t) = \theta(t,\tau_{s1}) \cdot \xi_1 \cdot \exp(-t/\tau_1) + \theta(t,\tau_{s2}) \cdot \xi_2, \quad (1)$$

where τ_{s1} and τ_{s2} are the decay and rise time constants of the step-like error functions, ξ_1 and ξ_2 are their amplitudes, and τ_1 is the decay constant (lifetime) of the decreasing component. The transient reflectivity at a probe wavelength of 400 nm decreases with a τ_{s1} of 0.28 ps after photoexcitation and recovers within 1–2 ps. An immediate decrease in the reflectivity is expected to be due to the state-filling effect occurring immediately after photoexcitation by the pump light leading to a decrease in the number of electrons transitioning from the valence band to the conduction band. The recovery occurs through relaxation of the excited electrons to the lowest energy level of the conduction band: the K- or Σ-valleys.[47–50] This behavior is very similar to that in a previous report.[51] The rise time constant of the step-like error function for the long-lived component, τ_{s2} can be fitted with any value between 0 and 2 ps. Because many linear and nonlinear contributions are involved in the long-lived component and the rise time cannot be precisely determined, we cannot connect this long-lived component to the ultrafast electronic scattering of excited electrons in the conduction band. Importantly, observing the time constant of the electronic scattering of excited electrons in the conduction band by simple transient reflectivity measurements is challenging because the signal is buried in complex linear and nonlinear contributions.

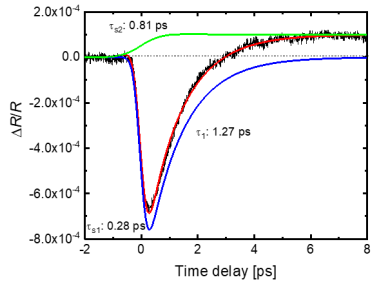

FIG. 4. Transient reflectivity at a probe light wavelength of 400 nm and an incident fluence of 5 mJ/cm^2.

In summary, we demonstrated ultrafast time-resolved electron diffraction measurements with double-optical-pulse excitation and ultrafast transient reflectivity measurements of 2H-$MoTe_2$ to understand the dynamics of excited electrons in the conduction band. By exploiting the Pauli blocking effect (saturable absorption), we observed electronic scattering in the conduction band using ultrafast time-resolved electron diffraction measurements with double-optical-pulse excitation. The excited electrons are scattered in terms of momentum within 100 fs. Ultrafast transient reflectivity measurements showed that the scattered electrons relax to the lowest energy valley (K- or Σ-valley) within 1–2 ps. Thermalization of the 2H-$MoTe_2$ lattice occurs more slowly through electron–lattice coupling within ~10 ps. Thus, the double pulse excitation in the Pauli blocking regime will be critical to understanding the electronic dynamics in the excited state, which gives insights into nonlinear optical effects. Note that one may access faster phase relaxation time constants by using faster excitation optical pulses (<35 fs),[52] which is essential for coherent control of electron systems in materials.

SUPPLEMENTARY MATERIAL

See supplementary material for sample preparation, intensity changes of the 100 and 200 diffraction spots with single- and double-pulse excitation, and intensity changes of the 100 and 200 diffraction spots with t_{pi} values of 0–20 ps.

ACKNOWLEDGMENTS

This work was supported by the Japan Society for the Promotion of Science (JSPS) Research Fellowships for Young Scientists, JSPS Kakenhi Grants-in-Aid (Nos. JP22KK0225, JP22KJ0352, and JP23H01101). This work was also supported by the Japan Science Technology Agent (JST) FOREST Program (No. JPMJFR211V) and CREST program (No. JPMJCR1875). Part of this work was carried out with the support of the National Institute for Materials Science (NIMS) Electron Microscopy Analysis Station, Nanostructural Characterization Group through the NIMS Open Facility (No. 22NM8222). We thank Ms. Koda at the Nanostructural Characterization Group for preparing the samples.

AUTHOR DECLARATIONS

Conflict of Interest

The authors have no conflicts to disclose.

DATA AVAILABILITY

The data that support the findings of this study are available from the corresponding author upon reasonable request.

REFERENCES

[1]K. F. Mak, C. Lee, J. Hone, J. Shan, and T. Heinz, *Phys. Rev. Lett.* **105**, 136805 (2010).

[2]W. G. Dawson, and D. W. Bullett, *J. Phys C: Solid State Phys.* **20**, 6159 (1987).

[3]D. H. Keum, S. Cho, J. H. Kim, D.-H. Choe, H.-J. Sung, M. Kan, H. Kang, J.-Y. Hwang, S. W. Kim, H. Yang, H. K. J. Chang, and Y. H. Lee, *Nat. Phys.* **11**, 482 (2015).

[4]K. Deng, G. Wan, P. Deng, K. Zhang, S. Ding, E. Wang, M. Yan, H. Huang, H. Zhang, Z. Xu, J. Denlinger, A. Fedorov, H. Yang, W. Duan, H. Yao, Y. Wu, S. Fan, H. Zhang, X. Chen, and S. Zhuo, *Nat. Phys.* **12**, 1105 (2016).

[5]M. Chhowalla, H. S. Shin, G. Eda, L. J. Li, K. P. Loh, and H. T. Zhang, *Nat. Chem.* **5**, 263 (2013).

[6]K. F. Mak, K. He, J. Shan, and T. Heinz, *Nat. Nanotechnol.* **7**, 494 (2012).

[7]E. J. Sie, J. W. McIver, Y. H. Lee, L. Fu, J. Kong, and N. Gedik, *Nat. Mater.* **14**, 290 (2015).

[8]N. Yoshikawa, K. Nagai, K. Uchida, Y. Takaguchi, S. Sasaki, Y. Miyata, and K. Tanaka, *Nat. Commun.* **10**, 3709 (2019).

[9]A. Chernikov, C. Ruppert, H. M. Hill, A. F. Rigosi, and H. F. Heinz, *Nat. Photon.* **9**, 466 (2015).

[10]S. Cho, S. Kim, J. H. Kim, J. Zhao, J. Seok, D. H. Keum, J. Baik, D.-H. Choe, K. J. Chang, K. Suenaga, S. W. Kim, Y. H. Lee, and H. Yang, *Science* **349**, 625 (2015).

[11]E. J. Sie, C. M. Nyby, C. D. Pemmaraju, S. J. Park, X. Shen, J. Yang, M. C. Hoffmann, B. K. Ofori-Okai, R. Li, A. H. Reid, S. Weathersby, E. Mannebach, N. Finney, D. Rhodes, D. Chenet, A. Antony, L. Balicas, J. Hone, T. P. Devereaux, T. F. Heinz, X. Wang, and A. M. Lindenberg, *Nature* 565, 61 (2019).

[12]T. Ichibayashi and K. Tanimura, *Phys. Rev. Lett.* **102**, 087403 (2009).

[13]J. Kanasaki, H. Tanimura, and K. Tanimura, *Phys. Rev. Lett.* **113**, 237401 (2014).

[14]U. De Giovannini, H. Hübener, and A. Rubio, *Nano Lett.* **16**, 7993 (2016).

[15]L. Wang, C. Xu, M.-Y. Li, L.-J. Li, and Z.-H. Loh, *Nano Lett.* **18**, 5172 (2018).

[16]Z. Chi, H. Chen, Q. Zhao, and Y.-X. Weng, *J. Chem. Phys.* **151**, 114704 (2019).

[17]T. Fukuda, K. Makino, Y. Saito, P. Fons, A. V. Kolobov, K. Ueno, and M. Hase, *Appl. Phys. Lett.* **116**, 093103 (2020).

[18] M. Cheng, S. Zhong, N. Rivas, T. Dekker, A. A. Petruk, P. Gicala, K. Pichugin, F. Chen, X. Luo, Y. Sun, A. W. Tsen, and G. Sciaini, *J. Phys. Chem. C* **126**, 13840 (2022).

[19]A. H. Zewail, *J. Phys. Chem. A* **104**, 5660 (2000).

[20]R. J. D. Miller, R. Ernstorfer, M. Harb, M. Gao, C. T. Hebeisen, H. Jean-Ruel, C. Lu, G. Moriena, and G. Sciaini, *Acta Crystallogr. A* **66**, 137 (2010).

[21]Y. Margalit, Y.-K. Lu, F. Ç. Top, and W. Ketterle, *Science* **374**, 976 (2021).

[22]K. Yonemitsu and K. Nasu, *Phys. Rep.* **465**, 1 (2008).

[23]S. Koshihara, T. Ishikawa, Y. Okimoto, K. Onda, R. Fukaya, M. Hada, Y. Hayashi, S. Ishihata, and T. Luty, *Phys. Rep.* **942**, 1 (2022).

[24]Z. H. Jin, P. Gumbsch, K. Lu, and E. Ma, *Phys. Rev. Lett.* **87**, 055703 (2001).

[25]R. Ernstorfer, M. Harb, C. T. Hebeisen, G. Sciaini, T. Dartigalongue, and R. J. D. Miller, *Science* **323**, 1033 (2009).

[26]S. Fanetti, N. Falsini, P. Bartolini, M. Citroni, A. Lapini, A. Taschin, and R. Bini, *J. Phys. Chem. Lett.* **10**, 4517 (2019).

[27]R. E. Russo, X. Mao, J. J. Gonzalez, V. Zorba, and J. Yoo, *Anal. Chem.* **85**, 6162 (2013).

[28]M. Hada, D. Zhang, K. Pichugin, J. Hirscht, M. A. Kochaman, S. A. Hayes, S. Manz, R. Y. N. Gengler, D. A. Wann, T. Seki, G. Moriena, C. A. Morrison, J. Matsuo, G. Sciaini, and R. J. D. Miller, *Nat. Commun.* **5**, 3863 (2014).

[29]U. Keller, K. J. Weingarten, F. X. Kärtner, D. Kopf, B. Braun, I. D. Jung, R. Fluck, C. Honninger, N. Matuschek, and J. Aus der Au, *IEEE J. Sel. Top. Quant.* **2**, 435 (1996).

[30]Z. Luo, D. Wu, B. Xu, H. Xu, Z. Cai, J. Peng, J. Weng, S. Xu, C. Zhu, F. Wang, Z. Sun, and H. Zhang, *Nanoscale* **8**, 1066 (2016).

[31]M. Liu, W. Liu, and Z. Wei, *J. Lightwave Technol.* **37**, 3100 (2019).

[32]T. Fukuda, U. Ozaki, S. Jeong, Y. Arashida, K. En-ya, S. Yoshida, P. Fons, J. Fujita, K. Ueno, M. Hase, and M. Hada. *J. Phys. Chem. C* **127**, 13149 (2023).

[33]M. Hada, D. Yamaguchi, T. Ishikawa, T. Sawa, K. Tsuruta, K. Ishikawa, S. Koshihara, Y. Hayashi, and T. Kato, *Nat. Commun.* 10, 4159 (2019).

[34]M. Hada, Y. Nishina, and T. Kato, *Acc. Chem. Res.* **54**, 731 (2021).

[35]G. Kresse, and J. Hafner, *Phys. Rev. B* **49**, 14251 (1994).

[36]P. E. Blöchl, *Phys. Rev. B* **50**, 17953 (1994).

[37]J. P. Perdew, A. Ruzsinszky, G. I. Csonka, O. A. Vydrov, G. E. Scuseria, L. A. Constantin, X. Zhou, and K. Burke, *Phys. Rev. Lett.* **100**, 136406 (2008).

[38]E. M. Mannebach, R. Li, K.-A. Duerloo, C. Nyby, P. Zalden, T. Vecchione, F. Ernst, A. H. Reid, T. Chase, X. Shen, S. Weathersby, C. Hast, R. Hettel, R. Coffee, N. Hartmann, A. R. Fry, Y. Yu, L. Cao, T. F. Heinz, E. J. Reed, H. A. Dürr, X. Wang, and A. M. Lindenberg, *Nano Lett.* **15**, 6889 (2015).

[39]M.-F. Lin, V. Kochat, A. Krishnamoorthy, L. Bassman, C. Weninger, Q. Zheng, X. Zhang, A. Apte, C. S. Tiwary, X. Shen, R. Li, R. Kalia, P. Ajayan, A. Nakano, P. Vashishta, F. Shimojo, X. Wang, D. M. Fritz, and U. Bergmann, *Nat. Commun.* **8**, 1745 (2017).

[40]A. Nakamura, T. Shimojima, Y. Chiashi, M. Kamitani, H. Sakai, S. Ishiwata, H. Li, and K. Ishizaka, *Nano Lett.* **20**, 4932 (2020).

[41]Y. Qi, M. Guan, D. Zahn, T. Vasileiadis, H. Seiler, Y. W. Windsor, H. Zhao, S. Meng, and R. Ernstorfer, *ACS Nano* **16**, 11124 (2022).

[42]J. Hu, Y. Xiang, B. M. Ferrari, E. Scalise, and G. M. Vanacore, *Adv. Funct. Mater.* **33**, 2206395 (2023).

[43]T. Fukuda, R. Kaburauchi, Y. Saito, K. Makino, P. Fons, K. Ueno, and M. Hase, *Phys. Status Solidi RRL* **16**, 2100633 (2022).

[44]P. Majchrzak, K. Volckaert, A. G. Čabo, D. Biswas, M. Bianchi, S. K. Mahatha, M. Dendzik, F. Andreatta, S. S. Grønborg, I. Marković, J. M. Riley, J. C. Johannsen, D. Lizzit, L. Bignardi, S. Lizzit, C. Cacho, O. Alexander, D. Matselyukh, A. S. Wyatt, R. T. Chapman, E. Springate, J. V. Lauritsen, P. D. C. King, C. E. Sanders, J. A. Miwa, P. Hofmann, and S. Ulstrup, *J. Electron. Spectros. Relat. Phenomena.* **250**, 147093 (2021).

[45]F. Liu, Q. Li, and X.-Y. Zhu, *Phys. Rev. B* **101**, 201405(R) (2020).

[46]F. Liu, *Chem. Sci.* **14**, 736 (2023).

[47]A. Britz, A. R. Attar, X. Zhang, H.-T. Chang, C. Nyby, A. Krishnamoorthy, S. H. Park, S. Kwon, M. Kim, D. Nordlund, S. Sainio, T. F. Heinz, S. R. Leone, A. M. Lindenberg, A. Nakano, P. Ajayan, P. Vashishta, D. Fritz, M.-F. Lin, and U. Bergmann, *Struct. Dyn.* **8**, 014501 (2021).

[48]W. Zheng, M. Bonn, and H. I. Wang, *Nano Lett.* **20**, 5807 (2020).

[49]J. Madéo, M. K. L. Man, C. Sahoo, M. Campbell, V. Pareek, E. L. Wong, A. Al-Mahboob, N. S. Chan, A. Karmakar, B. M. K. Mariserla, X. Li, T. F. Heinz, T. Cao, and K. M. Dani, *Science* **370**, 1199 (2020).

[50]E. J. Sie, T. Rohwer, C. Lee, and N. Gedik, *Nat. Commun.* **10**, 3535 (2019).

[51]J.-H. Kim, M. R. Bergren, J. C. Park, S. Adhikari, M. Lorke, T. Frauenheim, D.-H. Choe, B. Kim, H. Choi, T. Gregorkiewicz, and Y. H. Lee, *Nat. Commun.* **10**, 5488 (2019).

[52]K. Takubo, S. Banu, S. Jin, M. Kaneko, W. Yajima, M. Kuwahara, Y. Hayashi, T. Ishikawa, Y. Okimoto, M. Hada, and S. Koshihara, *Rev. Sci. Instrum.* **93**, 053005 (2022).